Review of Cellulose Nanocrystal-based Fluorophore Materials and Their Application in Metal Ion Detection

Ya Wang[1], Alain Dufresne[2], Peter R. Chang[3], XiaoZhou Ma[1,*], Jin Huang[1,*]

1. *School of Chemistry and Chemical Engineering, Joint International Research Laboratory of Biomass-Based Macromolecular Chemistry and Materials, Southwest University, Chongqing,* 400715*, China*

2. *Université Grenoble Alpes, CNRS, Grenoble INP, LGP2, F-*38000 *Grenoble, France*

3. *Bioproducts and Bioprocesses National Science Program, Agriculture and Agri-Food Canada,* 107 *Science Place, Saskatoon, SK, S7N0X2, Canada*

Abstract: Cellulose nanocrystals (CNCs), a unique and promising natural material extracted from native cellulose, have attracted considerable attention owing to their physical properties and special surface chemistry. This review focuses on chemical conjugation strategies that can be used for preparation of fluorescent-molecule labeled CNCs and the development of biomaterials. Furthermore, their application in the detection of metal ions and future development prospects are discussed. We hope to provide a clear view of the strategies for surface fluorescent modification of CNCs and their application in detection of metal ions.

Keywords: fluorescent cellulose nanocrystals; detection of metal ions; sensors; optical imaging; biomaterial

1 Introduction

The development of nanomaterials with sensing capability has grown over the past decade to meet the demand for applications in metal ion detection, drug delivery, and biological and biomedical sciences, as well as agricultural production[1-4]. In order to avoid potential environmental safety issues with nanomaterials and meet the need for renewable resource utilization, sustainable development and application of cellulose-based nanomaterials from renewable resources or waste materials have increasingly become a focus of research[5]. Cellulose is a linear homopolysaccharide that consisted of *D*-glucopyranose units linked by 1,4-β-linkages[6-7]. During biosynthesis, van der

Received: 23 July 2018; accepted: 16 August 2018.



Ya Wang, master candidate;
E-mail: wy0206@163.com



*Corresponding author:
XiaoZhou Ma, PhD;
E-mail: maxiaozhou@swu.edu.cn



*Corresponding author:
Jin Huang, professor; research interests: soft-matter chemistry and nanomaterials, especially novel materials derived from biomass resources;
E-mail: huangjin2015@swu.edu.cn

Waals and intermolecular hydrogen bonds between hydroxyl groups and the oxygens of adjacent molecules promote parallel stacking of multiple cellulose chains, forming basic fibers that further aggregate into larger microfibers[8]. These fibrils act as reinforcing elements in trees, plants, some marine organisms (tunicates), algae, and bacteria[9-11]. In these cellulose fibers, highly ordered (crystalline) structures of cellulose chains and disordered (amorphous) regions can be found. The crystalline regions contained within cellulose microfibers can be extracted to produce cellulose nanocrystals (CNCs)[12].

CNCs, which are also called cellulose nanowhiskers or nanocrystalline cellulose in some reports, exhibit special morphological, self-assembly, and modification ability properties. Fabricating new high-performance functional nanocomposites that can be applied in detection, diagnosis, or other biomedical applications is a frontier and a hot issue in cellulose-based research. Compared to inorganic nanoparticles, CNCs have many desirable properties and advantages, such as high crystallinity, a large surface area, high tensile strength and modulus, renewability, biodegradability, excellent colloidal stability, and facile modification[13]. CNCs are typically rod-like nanoparticles with a length of 100 nm to 1000 nm and a width of 20 nm to 100 nm[14-16]. CNCs can be isolated from a variety of cellulose sources, including plants (e.g., cotton, hemp, wood)[17-18], marine animals (e.g., tunicates)[19-21], bacteria (e.g., *Acetobacter xylinum*)[22], and so on, and also could be isolated from microcrystalline cellulose via mechanical shearing and acid and enzymatic hydrolysis[23-24]. The dimensions, crystal structure, degree of crystallinity, surface chemistry, morphology, and aspect ratio of the extracted CNCs depend strongly on the nature of the raw material and the reaction conditions. The most popular strategy for producing CNCs is to use acid hydrolysis, which can effectively remove the disordered or paracrystalline regions of the cellulose fiber while releasing CNCs with high crystallinity. Commonly, sulfuric acid[25-26], hydrochloric acid[27], phosphoric acid[28], and hydrogen bromide[29] can be used in this strategy to produce CNCs with different functional groups on their surfaces. The conditions of acid hydrolysis (e.g., the acid type and concentration, hydrolysis time, and temperature) will seriously affect the physical properties of the produced CNCs (i.e., the surface charge, size, yield, and birefringence). For example, CNCs obtained using sulfuric acid exhibit significantly lower thermal stability and higher stability in suspension than their counterparts obtained from hydrochloric acid.

On the one hand, CNCs exhibit favorable characteristics including biocompatibility, biodegradability, renewability, and nanoscale size; consequently, they have been used extensively to prepare sensing nanomaterials for applications in various fields[30]. The hydroxyl groups and large specific surface area of CNCs enable modification by physical or chemical reactions. CNCs have a large number of hydroxyl functional groups in their macromolecular chains, and owing to their high specific surface area, they can be easily modified via various reactions, such as carboxylation[31], esterification[32], silanization[33-34], cationic interaction[35], and graft copolymerization[36]. Chemical modification can introduce new functional groups or molecules onto the CNC surface while retaining the basic structure and properties of the particle[37]. For example, Dong et al introduced fluorescent molecules onto the CNC surface, and the fluorescent-tagged CNCs exhibited good potential for application in bioimaging and related diagnostics[38]. On the other hand, functional cellulose nanocrystalline materials are used as filler in polymers to produce high-performance nanocomposites[39-40], stimulus-responsive films[41-43], hydrogels[44], or photoinduced materials[45]. They are also used as templates for the synthesis of chiral[46], nematic[47], and porous materials, silica films, or TiO_2[48-49]. Furthermore, CNCs have been demonstrated to be biocompatible with living cells, thus they can also be used for *in vivo* testing[50].

Fluorescent molecules (small molecules or macromolecules) can be excited by light at a specific wavelength and radiate fluorescence at another wavelength that is different from the excitation

wavelength. Thus, fluorescent molecules are often used as sensors or indicators to detect target molecules. By introducing fluorescent molecules on the CNC surface, fluorescent CNCs (fCNCs) can be obtained, which can be dispersed in an aqueous solvent and display stable luminosity[51]. The wavelength of fCNCs depends strongly on the fluorescent molecules that have been grafted onto their surfaces. A wide range of fluorescent molecules or quantum dots (QDs) were grafted onto CNCs using different binding mechanisms. A common strategy to produce a fCNC sensor is to modify fluorescent molecules that can be used for detection onto its surface[52-55]. Many fluorescent indicators of heavy metal ions and transition metal ions such as Cu^{2+}, Hg^{2+}, Pb^{2+}, Cr^{3+}, and so on have been reported[56-60]. For example, Chen et al synthesized CNCs with porphyrin pendants (CNC-SA-$COOC_6$TPP) by a combination of carboxylation, extended esterification, and the dicyclohexylcarbodiimide reaction[61]. Owing to the good dispersion of fCNCs and the high selectivity and sensitivity of porphyrin derivatives, CNC-SA-$COOC_6$TPP can efficiently detect Hg^{2+} in water. CNCs were converted into fluorescent-labeled nanoparticles (Py-CNCs) by a three-step procedure. This sensing nanomaterial can be employed as a chemosensor for Fe^{3+} and for many applications in chemical, environmental, and biological systems[62].

Many reviews have summarized the surface modification and application of CNCs[5,10-11,50]. This review focuses on chemical conjugation strategies that can be used for the development of biomaterials using fluorescent-molecule-labeled CNCs. In the first part, the reactions used for fluorescence modification of CNCs are introduced. Then, by considering the differences among the molecules used to modify CNCs, the use of fCNCs for sensors is analyzed, and the detection mechanism is briefly introduced. Finally, a short summary and prospective are given.

2 Methods for surface chemical modification of CNCs

The surface chemistry of CNCs, especially the surface groups, is governed by the type of acid used for the hydrolysis procedure[37]. Because of the highly ordered arrangement of the crystalline structure, the reactivity of CNCs is different from that of a macromolecular polysaccharide, so they should not be simply regarded as multi-hydroxyl alcohols. The reactions between hydroxyl groups and a reagent occur only on the surface of CNCs (Fig.1). The preparation of fluorescent-tagged CNCs depends mainly on the chemical activity of functional groups on the surface of the CNCs and the resulting physical interaction. Typically, fCNCs are prepared mainly by the formation of covalent bonds between fluorophores and hydroxyl groups on the surface of CNCs, including esterification, etherification, amidation, the formation of a Schiff base, and the nucleophilic substitution reaction. The extraction and pre-chemical modification of CNCs for the preparation

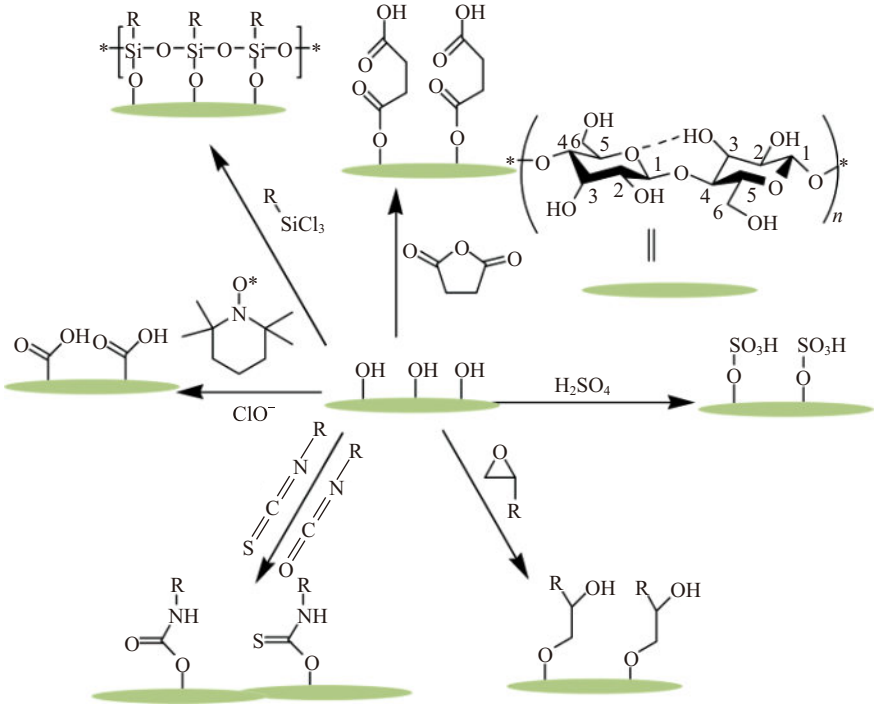


Fig.1 Common modification chemistries of CNC surfaces

of fCNCs are currently performed as follows.

Typical procedures for producing CNCs include the following steps:

(1) The cellulose raw material is purified under strict control of the temperature, stirring time, acid selection and concentration, and ratio of acid to cellulose. Subsequently, the pure cellulose material is hydrolyzed by a strong acid.

(2) Continuous centrifugation and repeated washing.

(3) Removal of free acid molecules by ultrafiltration.

(4) Concentration and drying of the suspension to obtain solid CNCs. The obtained CNCs are generally rod-shaped nanocrystals with a high aspect ratio.

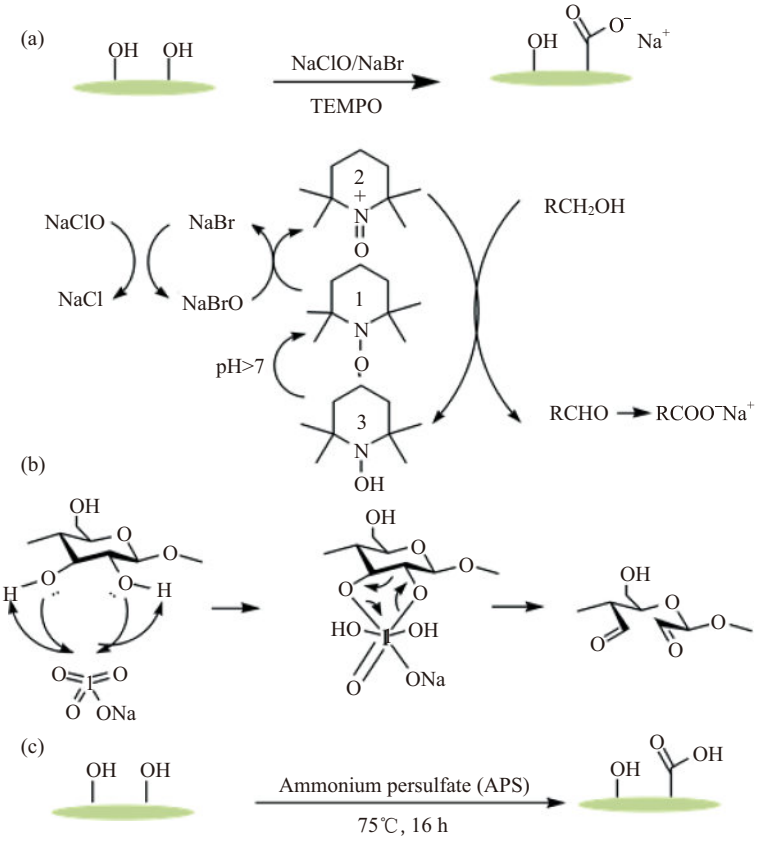
The hydroxyl groups on the CNC surface can be easily used to react with carboxyl groups or isocyanate groups on the fluorescent molecules. However, to conjugate fluorescent molecules that cannot be reacted with hydroxyl groups on the CNC surface, it is necessary to modify CNC with suitable functional groups, such as carboxyl groups or aldehyde groups. The CNC surface can be decorated with any of these groups via oxidation or esterification. Here, we will briefly discuss the mechanism of oxidation, a fundamental procedure for producing fCNCs.

A common strategy for oxidizing hydroxyl groups on the CNC surface is to use 2,2,6,6-tetramethylpiperidine-1-oxyl radical (TEMPO) as a catalyst to facilitate oxidation of the CNCs by NaClO[63-67]. The strategy can selectively oxidize C6—OH on the CNC surface into carboxyl groups. The mechanism is shown in Fig.2(a).

The oxidation process is pH-dependent and can be monitored using the pattern of aqueous NaOH consumption. In addition, in TEMPO/NaBr/NaClO oxidation of CNCs, the pH value of the reaction obviously affects the efficiency or the time required for oxidation. The optimum pH value for shortening the oxidation time was found to be 10[63].

The oxidized products have almost homogeneous chemical structures of β-1,4-linked polyglucuronic acid (cellouronic acid). Hence, the C6-primary hydroxyls of CNCs can be entirely converted to C6-sodium carboxyl or aldehyde groups by TEMPO-mediated oxidation, while the reaction also show a great selectivity to the C6-OH of CNC[70-72]. The maximum degree of oxidation (DOmax) of CNCs was calculated as 0.095 (roughly 0.1) using a simplified rectangle model. As the NaClO/anhydroglucose unit ratio changed, the DO of CNCs varied from partial oxidation (DO=0.029) to nearly complete oxidation (DO=0.097)[13, 73-74].

However, in TEMPO oxidation of CNCs, hypochlorite is used. Heating of hypochlorite in water can generate chlorine, which is extremely harmful for the environment; this can seriously limit the industrialization of the TEMPO oxidation process. APS is an inexpensive oxidant with low long-term toxicity and high water solubility[69,75] (Fig.2(c)). Persulfate oxidation is a novel method because the carboxylic acid



(a) Oxidation of CNCs by TEMPO[64]; (b) Oxidation of CNCs by sodium periodate[68]; (c) Oxidation of CNCs by APS[69]

Fig.2 TEMPO, sodium periodate, and APS oxidation of CNC surface

functionality is a direct result of the particle extraction method. Under heating, persulfate hydrolyzes in aqueous solution to form hydrogen peroxide and persulfate free radicals, which are strongly oxidizing. Under their combined action, the lignin, hemicellulose, and amorphous regions of cellulose in raw plant fiber materials are oxidized and degraded, thereby releasing the crystalline cellulose region. In addition, the persulfate method can effectively oxidize the hydroxyl groups on the surface of CNCs into carboxyl groups, increase the surface charge of CNCs, and enhance the colloidal stability of CNCs. Consequently, the resulting CNCs are uniform and possess nanoscale dimensions.

Sodium periodate is another useful oxidant that can be used to introduce aldehyde groups onto the CNC surface[31,41,68] (Fig.2(b)). It can selectively oxidize the C2 and C3 hydroxyl groups into 2,3-dialdehyde units. The resulting product is generally used to react with substances that have a primary amine group to form a Schiff base. For example, Alexa Fluor dyes can be facilely conjugated onto CNCs by this strategy while retaining the overall crystalline structure of the CNCs. The amino groups on Alexa Fluor dyes can form a Schiff base with the aldehyde groups on oxidized CNCs under mild conditions[77]. Further, 7-hydrazino-4-methylcoumarin (HMC) or 7-amino-4-methylcoumarin (AMC) can also be prepared by attaching hydrazine- or amino-substituted fluorophores onto CNCs to form hydrazine and Schiff-base compounds[78].

Anhydrides are a type of commonly selected reagent for esterification of the CNC surface (Fig.1). Mild conditions and controllable anhydride esterification were used to produce CNCs with a highly carboxylated ethylenediaminetetraacetic dianhydride (EDTAD)-modified surface (ECNCs), which are expected to maintain their integration, in contrast to those produced by TEMPO oxidation, for easy regulation of the densities of molecules. EDTAD can also be used for esterification of hydroxyl groups on the CNC surface. Acetic anhydride has been proved to be an effective reagent for acetylation of the CNC surface. Alkenyl succinic anhydride has also been used to improve the compatibility of CNCs with non-polar materials[79-80]. Via esterification, the modified CNCs can achieve a higher carboxylation degree than TEMPO-oxidized CNCs and can be used to make fCNCs with higher fluorescence intensity. The application of these reactions in the preparation of fCNCs will be introduced in detail in the following section.

3 Methods of preparing fluorescent–tagged CNCs

Owing to the various functional groups on fluorescent molecules (small molecules or macromolecules) or QDs, e.g., the isocyanate group, carboxyl group, amino group, hydrazine group, and alkynyl group, many types of reactions can be applied. Thus, fCNCs can form chemical or physical interactions between fluorescent molecules or QDs and the surface-active groups of the CNCs. Here, we will focus mainly on methods of constructing fCNCs. Table 1 summarizes recent studies on surface immobilization of fluorescent molecules (small molecules or macromolecules) or QDs on CNCs using different strategies (chemical binding or physical absorption).

3.1 Carbamation reaction

Isocyanate or isothiocyanate can react with hydroxyl groups or amino groups on the surface of CNCs[38,96-97,99]. This reaction is typically used to modify the CNC surface with fluorescent molecules or other functional groups. Therefore, this reaction is very suitable for CNC surface modification in some cases. However, the base used in this reaction may damage biomacromolecules such as proteins, so the use of the resulting CNCs in living organisms is limited. In 2007, Roman's group reported a three-step strategy for covalently attaching fluorescein-5′-isothiocyanate (FITC) molecules to the surface of CNCs[38,99]. First, epichlorohydrin was attached to the hydroxyl groups of CNCs by nucleophilic substitution. Subsequently, ammonium hydroxide was used to convert the epoxy group to an amino group. Finally, FITC was conjugated onto CNCs via the reaction between the isothiocyanate group and amino group. It was shown that the unlabeled

Table 1 Fluorescent tagging of CNCs

Type	Processing method	Fluorophore	Binding mechanism	Applications	Ref.
CNC	Sulfuric acid hydrolysis	Coumarin-3 -carboxylic acid and carbazole -9-yl-acetic acid	Esterification	Bioimaging, biosensors, phototherapy	[81]
		Rhodamine B isothiocyanate (RBITC)	Carbamation	Bioimaging	[82]
		Alexa Fluor 546	Nucleophilic substitution	Bioimaging	[77]
		Terpyridine		Ion detection	[83]
		Poly(N-Isopropylacrylamide) (PNIPAAM)	ATRP	Drug release	[84-85]
		P(AzoC6MA-co-DMAEMA)		Sensor	[86]
		Poly (amidoamine)	Amidation	Sensor	[87]
		Imidazolium	Click chemistry or physical absorption	Ion exchange	[88]
		CdSe QDs		Biomedical	[89]
	Desulfated/HCl hydrolysis	5-(4, 6-dichlorotriazinyl) aminofluorescein (DTAF)	Nucleophilic substitution	Optical markers	[90]
CNC-COOH	TEMPO-mediated oxidation	Rhodamine (RhB)	Amidation	Temperature sensor	[91]
		Carbon quantum dots		*In vitro* bioimaging	[92]
		Coumarin and anthracene	Click chemistry	Sensor	[93]
	Persulfate oxidation	CdSe/ZnS quantum dots	Amidation	Optical bioimaging	[76]
	Anhydride esterification	7-amino-4-methylcoumarin (AMC)	Amidation	Ion detection	[80]
		porphyrin pendants	Esterification	Ion detection	[61]
CNC-CHO	Sodium periodate	Alexa Fluor 546/663	Schiff base reaction	Bioimaging	[77,94]
		7-hydrazino-4-methylcoumarin and 7-amino-4-methylcoumarin			[78]
CNC-NH_2	Silanization	1-pyrenebutyric acid N-hydroxy succinimide ester (PSE) or FITC	Carbamation	Bioimaging	[95]
		FITC			[96]
	Esterification and thiol-ene click	Fluorescein isothiocyanate (FITC) and Rhodamine B isothiocyanate (RBITC)	Amidation	Sensor materials or tissue engineering	[97]
		5 (and 6)-carboxy-2′,7′-dichlorofluorescein (CDCF)		Drug delivery	[98]
	Ring opening reaction	RBITC and FITC	Carbamation	Bioimaging and drug delivery	[99]
		FITC		Bioimaging	[38,100]
		Pyrene	Nucleophilic substitution	Ion detection	[62]
		Graphene quantum dots	Amidation	Biomedical	[101]

suspension was colorless and slightly opaque, whereas the FITC-labeled CNC suspension appeared clear and yellow. Further, according to the results of UV/vis spectroscopy, the FITC-labeled nanocrystals showed the absorption maxima peak associated with both the dianionic (490 nm) and anionic (453 and 472 nm) forms of FITC, whereas unlabeled CNCs did not show any absorption peak in the wavelength range 200~600 nm. A calculation showed that approximately 30 μmol/g of FITC was attached to each CNC, which was sufficient for application in bioimaging.

The method of modifying the surface of CNCs with two fluorescent molecules (FITC and RBITC) separately is similar to that described above[99-100]. A suspension of RBITC-labeled CNCs appeared wine red and exhibited emission under excitation at 540 nm, which is attributed to RBITC. Note that in comparison with a free RBITC aqueous solution, the fluorescence emission of RBITC-labeled CNCs was red-shifted (from 577 nm to 584 nm), which was attributed to

the influence of the fluorescent molecules covalently attached to the nanocrystals. Although both molecules showed low cytotoxicity and strong fluorescence, further study demonstrated that FITC-CNCs and RBITC-CNCs were unsuitable for use as biomarkers. Compared to FITC-CNCs, RBITC-CNCs penetrated the cell membrane more easily at various pH values owing to their cationic surfaces. However, the FITC-CNCs could penetrate the cell membrane only at low pH values but aggregated on the cell surface in neutral and high pH environments, allowing the FITC-CNCs to better detect cancer cells.

Nielsen et al[97] developed two synthetic approaches to introduce two fluorescent or dye molecules onto CNCs for the preparation of dual-fluorescent-labeled CNCs. The first approach employed a procedure similar to that of Dong and Roman and involved the reaction between amino CNCs and both isothiocyanates, FITC and RBITC. The quantities of FITC and RBITC on the dual-fluorescent-labeled CNCs were estimated to be 2.8 μmol/g and 2.1 μmol/g, respectively. To avoid the use of scarce isothiocyanate fluorescent molecules, a new three-step procedure was performed on CNCs: the introduction of a double bond on the CNCs via esterification, followed by thiol-ene Michael addition and finally coupling with succinimidyl ester dyes. Two different pH-sensitive dyes, 5-(and-6)-carboxyfluorescein succinimidyl ester (FAM-SE) and Oregon green 488 carboxylic acid, succinimidyl ester (OG-SE), were grafted onto CNCs along with the reference, fluorophore 5,6-carboxytetramethyl rhodamine succinimidyl ester (TAMRA-SE) dye, which is brighter than Rhodamine B and is available only as a succinimidyl ester. The average quantities of the dyes on the labeled CNCs were 10.4 μmol/g (FAM-SE), 4.7 μmol/g (TAMRA-SE) and 7.3 μmol/g (OG-SE), 4.2 μmol/g (TAMRA-SE), respectively. The dual-fluorescent-labeled CNCs (FITC- and RBITC-labeled CNCs) and two dual-dye-labeled CNCs (FAM-SE- and TAMRA-SE-labeled CNCs as well as OG-SE- and TAMRA-SE-labeled CNCs) all exhibited pH sensing in McIlvaine buffers under various pH value conditions.

3.2 Nucleophilic substitution

Nucleophilic substitution is another strategy for modifying the surface of CNCs with fluorescent molecules[62,81,102-103]. Fluorescent molecules containing halogen atoms such as chlorine or bromine are generally more suitable for this strategy. Hydroxyl groups or amino groups on the surface of CNCs (modified by an amination reaction) act as a nucleophilic reagent and react with a bromomethyl group or a chloromethyl group on a fluorescent molecule and replace a halogen atom by a nucleophilic substitution reaction; thus, CNCs can be modified by functional molecules. Both carbazole[81] and pyrene[62] were introduced onto the CNC surface by this reaction. Furthermore, by using this strategy, 5-(4,6-dichlorotriazinyl) amino-fluorescein (DTAF) and RBITC were also attached to the CNC surface in an alkaline environment in one step[90]. Although the requirements for the reagents and environment are relatively high, this method of grafting fluorescent molecules onto the surface of CNCs is simple[62,102].

3.3 Amidation reaction

In some studies, many different molecules were grafted onto nanocrystals using the carboxylation-amidation reaction to create a covalent amide bond between a primary amine-terminated molecule and carboxylated CNCs by COOH-NH_2 coupling[67,74,104-106]. It was reported that during this reaction, to make conjugation easier, N-hydromaleimide (NHS) and 1-ethyl-3-(3-dimethylaminopropyl) carbodiimide can be used to activate the carboxyl group and facilitate the reaction between the carboxyl and primary amine in the first step (Fig.3). Then, the NHS-activated carboxyl group is directly reacted with the amine group in a neutral or alkaline environment to form the amide. By using this two-step reaction, the amidation reaction can be controlled, and no excess byproducts are produced. The advantages of this method are mild reaction conditions, a simple operation procedure, and convenient disposal. Amidation can be applied to studies in which rhodamine methacrylamide is immobilized on the surface of the

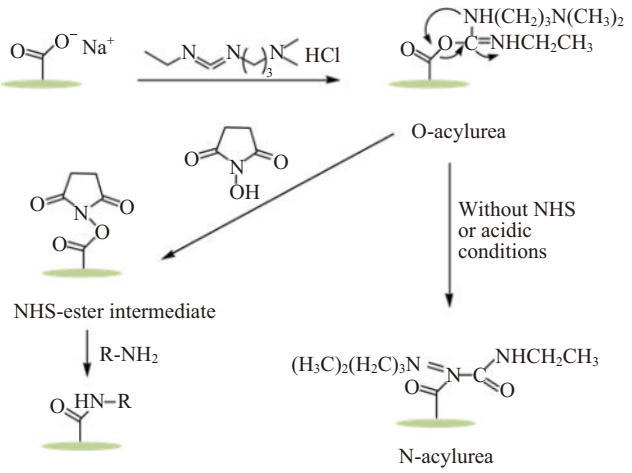


Fig.3 Amidation on CNC surface

CNC[61,76,91,98] (Fig.4(c) and Fig.4(e)). Rhodamine, a popular fluorophore probe, has been investigated in terms of its physical and chemical features owing to its excellent photophysical properties and low cost. Because rhodamine methacrylamide is heat-sensitive, the fluorescence signal of rhodamine-methacrylamide-modified CNCs (RhB-CNCs) can be controlled, because the isoporphyrin-a substructure destroys the binding of rhodamine and turns the fluorescence signal off. When RhB-CNCs are treated with ultraviolet light, the five-membered open ring re-forms the π bond and turns the fluorescence signal on. Huang's group reported the use of the amino acid L-leucine as a spacer linker for attachment of 5 (and 6)-carboxy-2', 7'-dichlorofluorescein to CNCs[98].

3.4 Schiff base reaction

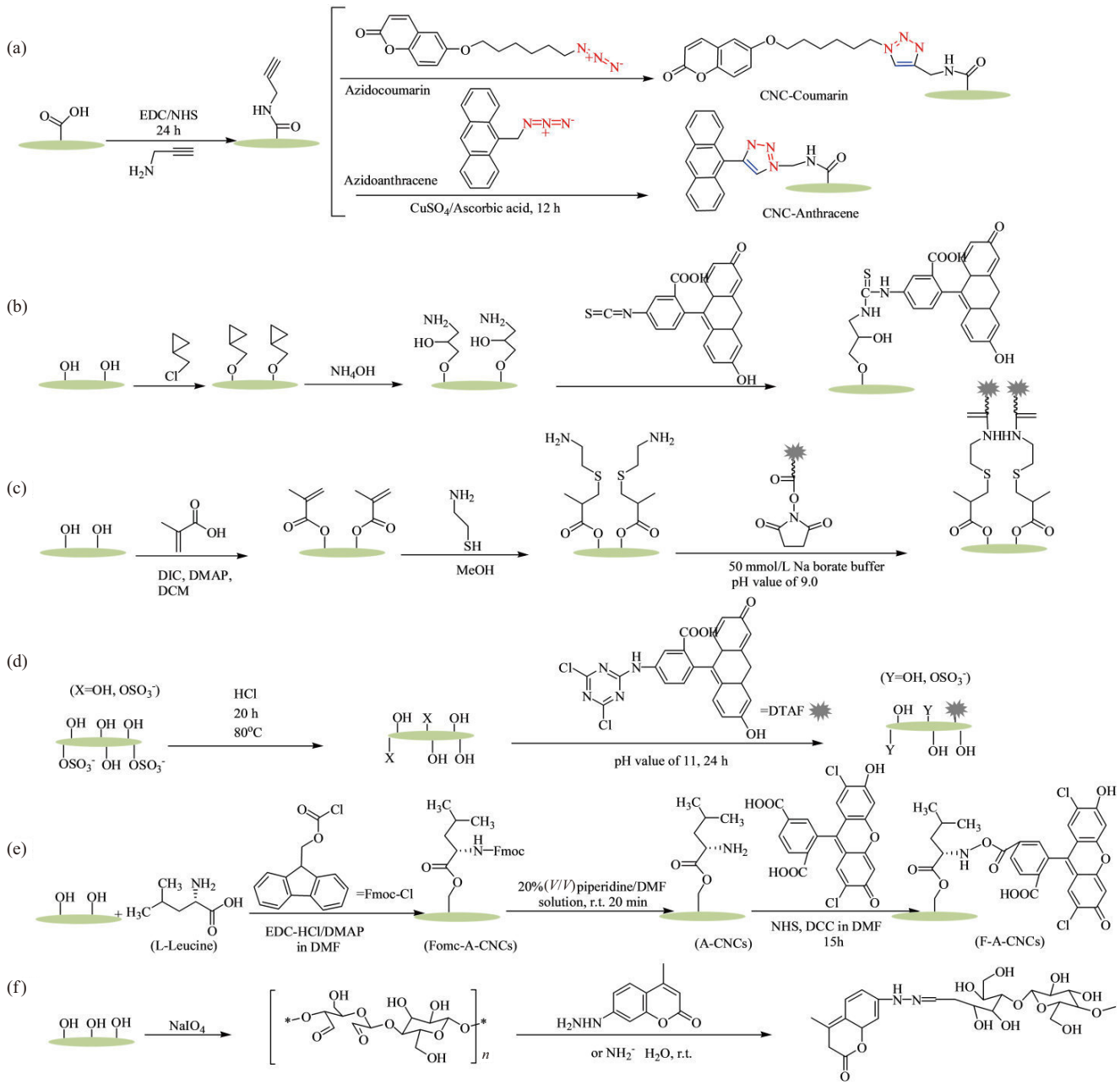
A Schiff base is a compound in which carbon atoms and nitrogen atoms are bonded by double bonds. Although the formation of Schiff bases is reversible, the reaction is widely used for surface modification of CNCs[77-78,82,94] (Fig.4(f)). Reduction of a double bond between a carbon atom and a nitrogen atom into a single bond is a useful measure to immobilize a functional group on the surfaces of CNCs. However, because the glucoside at the end of the cellulose chain can form an aldehyde group, it may be much easier to decorate the CNC surface with a functional group using a Schiff base. The degree of substitution (DS) of the fluorescent-molecule-modified CNC obtained by this strategy is relatively low, but the reaction can be carried out in one step and stably under physiological conditions, and thus it is still used for some *in vivo* biomarkers. Huang et al used this strategy for fluorescent labeling of CNCs with HMC and AMC[78]. CNCs labeled with Alexa Fluor 633 were also prepared by this reaction[93].

3.5 Click reaction

Click chemistry has been utilized to prepare new fluorescent cellulose nanomaterials[88-89,94] (Fig.4(a)). Filpponen et al reported that the primary hydroxyl groups in CNCs were first selectively oxidized to carboxylic acids. In the next step, a compound having a terminal amine functional group (propargylamine) was grafted to the surface of the oxidized CNCs by an amidation reaction, and the alkynyl group was used as a reaction site for further modification. These surface-modified CNCs were finally subjected to click chemistry reaction conditions, that is, copper(I)-catalyzed azide-alkyne cycloaddition with an azide-containing fluorescent coumarin, to produce highly fluorescent-tagged CNCs[94].

4 Fabrication of fluorescent CNCs for ion detection

Among many green nanomaterials, CNCs are preferred owing to their excellent properties, such as the high density of surface active hydroxyl groups and low cost[22,37,69,107]. In addition, an important property of CNCs prepared by sulfuric acid hydrolysis is the grafting of sulfate esters, which are negatively charged, onto the surfaces of the CNCs. Owing to the presence of charged groups, the colloidal stability of aqueous suspensions of CNCs helps to block aggregation through electrostatic repulsion interactions[26]. This property is attractive for water-based dispersion and processing of CNCs. There are many reports on microcrystalline cellulose[53-54], fluorophore-labeled cellulose[55], and CNCs. This review will consider mainly works related to CNCs. In covalent conjunction with CNCs, fluorescent molecules (small molecules or macromolecules) or QDs can be used to label CNCs not only for fluorescence bioassay and bioimaging



(a) Click chemistry[93]; (b) Carbamation[38]; (c) (e) Amidation[97-98]; (d) Nucleophilic substances[90,102]; (f) Schiff base reaction[78]

Fig.4 Schematic representation of the synthesis of fluorescent CNCs and the results

applications but also for the detection of metal ions and monitoring the bio-effects of nanoparticles inside cells or human beings. Owing to the small size of fluorescent molecules (which results in smaller spatial effects) and their higher reactivity (various functional groups and stable chemistry), it is easier to bind fluorescent molecules to the CNC surface than other macromolecules. Dong and Roman used a multistep method to tag NH_2-CNCs with FITC at a level of one fluorophore group per 27 nm^2 of CNC surface[38]. Mahmoud et al used a similar method to tag CNCs with fluorophores, including FITC and RBITC[99]. A simple, low-cost, and scalable two-step method was used to attach FITC and a pyrene-based fluorophore to aminosilane-treated CNCs[95-96]. Filpponen et al used TEMPO oxidation, carbodiimide amidation, and copper (I)-catalyzed azide–alkyne click chemistry to add coumarin and anthracene fluorophores

to CNC surfaces[93]. Nielsen et al presented a thiol-ene reaction method to modify CNCs with pH-responsive fluorophores[97]. Abitbol et al prepared DTAF-tagged CNCs by nucleophilic substitution[90]. In addition, stimuli-responsive fluorescent sensors are also widely applied in the regulation of cell or tissue environments and other fields. Stimuli-responsive polymers have attracted attention in recent years. Yuan et al synthesized CNC-g-poly(AzoC_6MA-co-DMAEMA) fluorescent nanosensors by the atom transfer radical copolymerization (ATRP) reaction[86]. In contrast to organic fluorophores, core-shell QDs are resistant to photobleaching and have high quantum yields, broad excitation, and narrow, symmetric emission bands[46, 76]. The size-dependent optical properties allow simultaneous excitation of QDs of different sizes using a single wavelength, such as simple UV light[92, 101, 108]. The interest in cellulose as a substrate for fluorescent molecules and nanoparticles is driven by its relative inertness, along with recognition of the potential of this combination to develop new functional materials that combine the unique optical properties of QDs with the properties contributed by cellulose, e.g., transparency, good mechanical properties, and self-assembly. Abitbol et al used a carbodiimide chemistry coupling approach to decorate carboxylated CNCs with Cd/ZnS QDs[76]. These fluorescent-group-modified nanomaterials are used in bioimaging, sensing, *in vivo* detection, and so on. Optical nanosensors are widely used today, and many of them use fluorescence as an indicator to measure changes in biological indicators owing to their high sensitivity, usefulness for remote monitoring, and real-time performance.

Chen et al synthesized a porphyrin-functionalized CNC fluorescence nanosensor (CNC-SA-$COOC_6$TPP) by simple esterification of extended porphyrin (TPPC_6-OH) with carboxylated CNCs (CNC-SA-COOH) (Fig.5)[61]. Owing to the specific formation of the Hg^{2+}-porphyrin complex as well as the interaction stoichiometry of one Hg^{2+} per porphyrin moiety, Hg^{2+} was specifically detected with interference from other metal ions[109-113]. Porphyrin pendants could serve

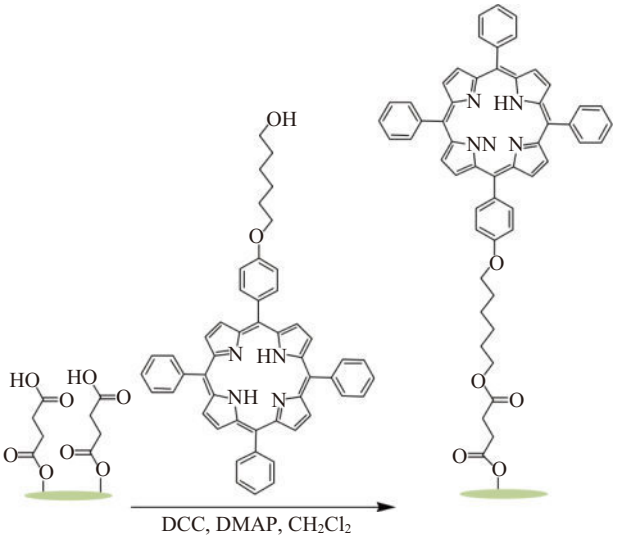


Fig.5 Synthesis of CNC-SA-$COOC_6$TPP[61]

as Hg^{2+}-reactive sensors, and the CNCs afforded mechanical support, acting as a backbone with good dispersion in water. Moreover, the CNC-SA-$COOC_6$TPP nanomaterials could be easily separated from water by filtering. These features make CNC-SA-$COOC_6$TPP nanomaterials a promising fluorescent chemical sensor. The synthesized chemical sensor realized high-selectivity detection of Hg^{2+} with a credible detection limit of 5.0×10^8 mol/L (50 nmol/L) at a concentration of 0.01 wt%. When combined with Hg^{2+}, the CNC-SA-$COOC_6$TPP nanomaterials exhibited a distinct blue shift of the fluorescence peak from 652.5 nm to 628.5 nm, which was assigned to stable coordination aggregates induced by Hg^{2+}[114].

Fluorescent sensors for Fe^{3+} in aqueous environments are rare. A limiting factor in the design of such sensor molecules is the paramagnetism of Fe^{3+}, which can cause fluorescence quenching[97, 115]. In addition, many Fe^{3+}-selective fluorescent probes are hydrophobic, and this incompatibility with aqueous environments limits the use of these sensors in biological systems. To overcome fluorescence quenching, researchers utilized a "green" nanomaterial for this template. The fluorescent chromophore, pyrene, which can detect Fe^{3+}, is grafted onto the surface of CNC to improve the compatibility of the chromophore with aqueous environments. CNCs grafted with pyrene (Py-CNCs) are well dispersed in water (Fig.6). The

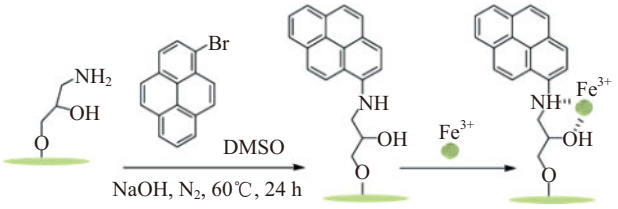
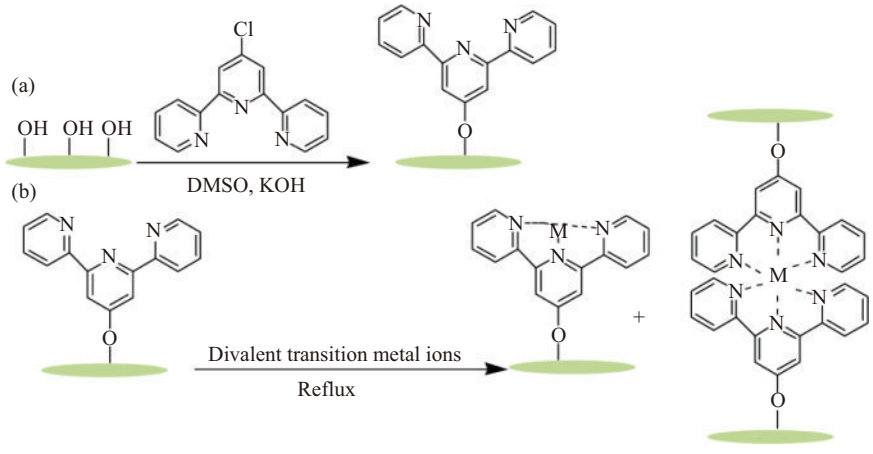


Fig.6 Fluorescence labeling of CNCs with pyrene dyes and the coordination mechanism of Fe^{3+} for Py-CNCs[62]

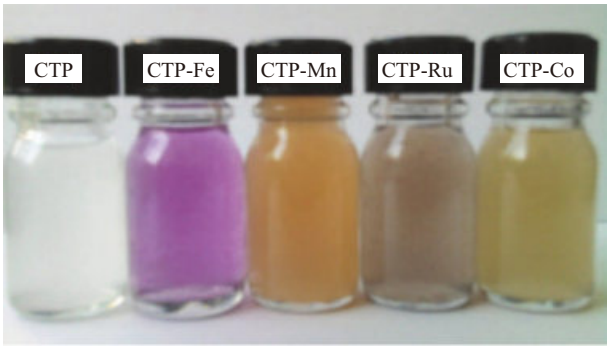
sensors were used to detect Fe^{3+} in environmental and biological systems[62]. The fluorescence emission of pyrene was enhanced after modification of CNCs. The Py-CNCs exhibited high selectivity toward Fe^{3+} among other screened metal ions, with good discrimination between different iron oxidation states (Fe^{2+} and Fe^{3+}). The quenching reaction mechanism of Fe^{3+} on Py-CNC is ligand-metal charge transfer, in which the charge transfer transition is initiated by the unfilled shell of paramagnetic and iron ions. The coordination reaction between Fe^{3+} and Py-CNCs is mainly an additional coordination of the N—H group, which is well known for strong binding affinity for transition metals and 2-hydroxy groups[56, 116].

Terpyridine is a N heterocycle that has a strong binding affinity for many transition metal ions owing to its ability to chelate with the dπ-pπ* of the coordination metal ions[117-119]. Much research has been done on the use of transition metal-terpyridine complexes in optics, electricity, magnetism, etc., and this complex can be reversed



Reprinted with permission from Ref.[83]; Copyright (2012) Taylor & Francis.

Fig.7 (a) Reaction of CTP nanocrystal formation, (b) reaction of CTP with divalent transition metal ions[83]



* From left to right: CTP, CTP-Fe(II), CTP-Mn(II), CTP-Ru(III), and CTP-Co(II)[53].

Fig.8 Dilute suspensions of CTP complexes with different transition metal ions as they appear in normal light

by changing the pH value or temperature[103, 120-121]. CNCs were used as a potential scaffold for the construction of ordered arrays and networks with tunable properties. Terpyridine-modified CNCs (CTP), a new metallo- and supramolecular nanocellulosic material[122-123], is prepared by nucleophilic substitution (Fig.7(a)), and its corresponding transition metal complexes have unique physicochemical properties and offer the possibility of forming supramolecular derivatives with a wide range of functionalities and applications (Fig.7(b)). According to the valence and reactant ratio, CTP can form a mono- or bis-teridinium metal complex with different transition metal ions. The complexation of transition metal ions with CTP occurs instantaneously, resulting in the formation of metal-nanocellulose materials with different optical properties (Fig.8). Owing mainly to complexation with different transition metal ions, the apparent red shift of the π-π* absorption band of terpyridine is from 350 nm to 413 nm.

Coumarin derivatives are important fluorescent dyes with high photoluminescence quantum efficiencies and applications in optical materials; they also display antitumor, antiviral, and antioxidant properties. Because the carbon in the 3-position in coumarins has a partial negative charge, the intramolecular

charge transfer (ICT) mechanism can be modulated by introducing an electron-donating substituent at the 7-position or an electron-withdrawing substituent at the 3-position. Attachment of a hydrazide chain to the coumarin moiety at the 3-position could both enhance the ICT and set up a selective donor set for copper via the carbonyl oxygen and amide nitrogen[124, 125]. Huang et al constructed a new type of coumarin-modified CNC probe for selective and quantitative detection of Cu^{2+} in solution via a two-step reaction strategy, i.e., esterification of EDTAD to produce CNCs with a highly carboxylated surface and subsequent amidation with AMC to give fluorescent AMC-amidated ECNCs (Fig.9). At the same time, the steric effect and colloidal stability of rigid fCNCs might contribute to the prevention of self-quenching of surface AMC, resulting in a stable fluorescence intensity regardless of the fCNC concentration[80].

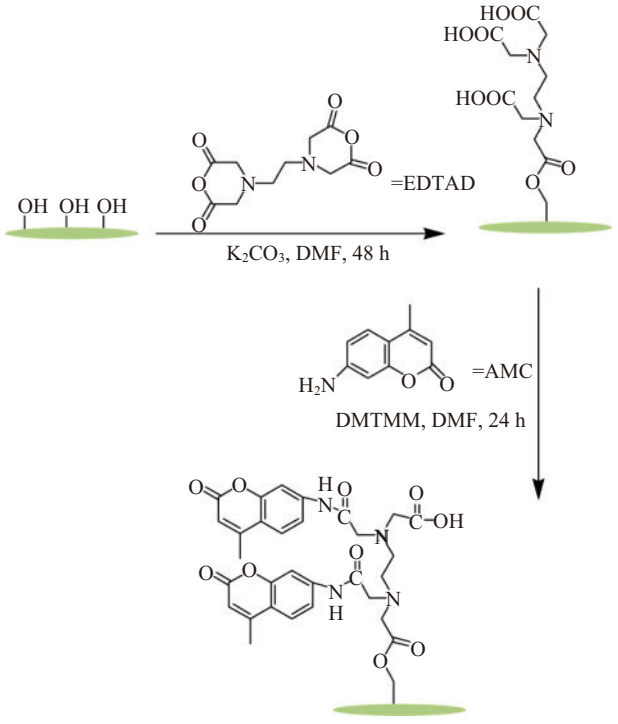


Fig.9 Schematic illustration of molecular-level structural changes on the CNC surface during synthesis of fCNCs

5 Conclusions

In this review, we focused on fCNC-based metal ion detection. Strategies for surface modification of CNCs, an important step in preparation of fCNCs, were first introduced. Then, various works that used the rich hydroxyl groups on the CNC surface to prepare fCNCs with different emission wavelengths and luminous behavior were reviewed. Finally, we analyzed works on metal ion detection by fCNCs in detail, gave examples, and discussed the effect of the molecular structure of fCNCs on their detection ability. Compared with fluorescent-molecule-based metal ion detection, detection by fCNCs has advantages, as follows: 1) Because the raw material of fCNCs, CNCs, have hydrophilic surface, fCNCs can be stably dispersed in water, so they provide an ideal platform to detect metal ions in aqueous solution; 2) The facile surface modification of CNCs can provide more options for designing fCNC sensors; 3) fCNCs exhibit stable fluorescence intensity with respect to the fCNC concentration, and thus provide a reliable detection result. Thus, in conclusion, owing to the low toxicity and low cost of CNCs, fCNCs are expected to afford high-performance but inexpensive and environmentally friendly sensors with specific functional properties for *in vivo* detection, bioimaging, drug delivery, and so on.

Acknowledgments

Authors are grateful to the National Natural Science Foundation of China (51373131), Fundamental Research Funds for the Central Universities (XDJK2016A017 and XDJK2016C033), Project of Basic Science and Advanced Technology Research, Chongqing Science and Technology Commission (cstc2016, jcyjA0796), and the Talent Project of Southwest University (SWU115034). LGP2 is part of the LabEx Tec 21 (Investissements d'Avenir-grant agreement n° ANR-11-LABX-0030) and of the PolyNat Carnot Institut (Investissements d'Avenir-grant agreement n° ANR-11-CARN-030-01).

References

[1] Persin Z, Stana-Kleinschek K, Foster T J, et al. Challenges and opportunities in polysaccharides research and technology: The EPNOE views for the next decade in the areas of materials, food and health care[J]. Carbohydrate Polymers, 2011, 84(1): 22-32.

[2] Xuan L, Zhang P, Li X, et al. Trends for nanotechnology development in China, Russia, and India[J]. Journal of Nanoparticle Research, 2009, 11 (8): 1845-1866.

[3] Baruah S, Dutta J. Nanotechnology applications in pollution sensing and degradation in agriculture: a review[J]. Environmental Chemistry Letters, 2009, 7(3): 191-204.

[4] Ruiz-Palomero C, Soriano M L, Valcárcel M. Nanocellulose as analyte and analytical tool: Opportunities and challenges[J]. Trac Trends in Analytical Chemistry, 2017, 87: 1-18.

[5] Siqueira G, Bras J, Dufresne A. Cellulosic bionanocomposites: A review of preparation, properties and applications[J]. Polymers, 2010, 2(4): 728-765.

[6] Gopalan Nair K, Dufresne A, Gandini A, et al. Crab shell chitin whiskers reinforced natural rubber nanocomposites. 3. Effect of chemical modification of chitin whiskers[J]. Biomacromolecules, 2003, 4(6): 1835-1842.

[7] Gopalan Nair K, Dufresne A. Crab shell chitin whisker reinforced natural rubber nanocomposites. 2. Mechanical behavior[J]. Biomacromolecules, 2003, 4(3): 666-674.

[8] Yoshiharu N. Structure and properties of the cellulose microfibril[J]. Journal of Wood Science, 2009, 55(4): 241-249.

[9] Nishiyama Y, Langan P, Chanzy H. Crystal structure and hydrogen-bonding system in cellulose Iα from synchrotron X-ray and neutron fiber diffraction[J]. Journal of the American Chemical Society, 2003, 125(47): 14300-14306.

[10] Habibi Y, Lucia L A, Rojas O J. Cellulose nanocrystals: chemistry, self-assembly, and applications[J]. Chemical Reviews, 2010, 110(6): 3479-3500.

[11] Moon R J, Martini A, Nairn J, et al. Cellulose nanomaterials review: structure, properties and nanocomposites[J]. Chemical Society Review, 2011, 40(7): 3941-3994.

[12] Lin N, Huang J, Dufresne A. Preparation, properties and applications of polysaccharide nanocrystals in advanced functional nanomaterials: a review[J]. Nanoscale, 2012, 4(11): 3274-3294.

[13] Habibi Y, Chanzy H, Vignon M R. TEMPO-mediated surface oxidation of cellulose whiskers[J]. Cellulose, 2006, 13(6): 679-687.

[14] Chen J, Lin N, Huang J, et al. Highly alkynyl-functionalization of cellulose nanocrystals and advanced nanocomposites thereof via click chemistry[J]. Polymer Chemistry, 2015, 6(24): 4385-4395.

[15] Van d B O, Capadona J R, Weder C. Preparation of homogeneous dispersions of tunicate cellulose whiskers in organic solvents[J]. Biomacromolecules, 2007, 8(4): 1353-1357.

[16] Favier V, Chanzy H, Cavaille J Y. Polymer nanocomposites reinforced by cellulose whiskers[J]. Macromolecules, 1995, 28(18): 6365-6367.

[17] Sacui I A, Nieuwendaal R C, Burnett D J, et al. Comparison of the properties of cellulose nanocrystals and cellulose nanofibrils isolated from bacteria, tunicate, and wood processed using acid, enzymatic, mechanical, and oxidative methods[J]. ACS Applied Materials & Interfaces, 2014, 6(9): 6127-6138.

[18] Ditzel F I, Prestes E, Carvalho B M, et al. Nanocrystalline cellulose extracted from pine wood and corncob[J]. Carbohydrate Polymers, 2017, 157: 1577-1585.

[19] Cao L, Fu X, Xu C, et al. High-performance natural rubber nanocomposites with marine biomass (tunicate cellulose) [J]. Cellulose, 2017, 24(7): 2849-2860.

[20] Jorfi M, Roberts M N, Foster E J, et al. Physiologically responsive, mechanically adaptive bio-nanocomposites for biomedical applications[J]. ACS Applied Materials & Interfaces, 2013, 5(4): 1517-1526.

[21] Shanmuganathan K, Capadona J R, Rowan S J, et al. Stimuli-responsive mechanically adaptive polymer nanocomposites[J]. ACS Applied Materials & Interfaces, 2010, 2(1): 165-174.

[22] Vasconcelos N F, Feitosa J P, da Gama F M P, et al. Bacterial cellulose nanocrystals produced under different hydrolysis conditions: Properties and morphological features[J]. Carbohydrate Polymers, 2017, 155: 425-431.

[23] Siqueira G, Tapin-Lingua S, Bras J, et al. Morphological investigation of nanoparticles obtained from combined mechanical shearing, and enzymatic and acid hydrolysis of sisal fibers[J]. Cellulose, 2010, 17(6): 1147-1158.

[24] Filson P B, Dawson-Andoh B E, Schwegler-Berry D. Enzymatic-mediated production of cellulose nanocrystals from recycled pulp[J]. Green Chemistry, 2009, 11(11): 1808-1814.

[25] Roman M, Winter W T. Effect of sulfate groups from sulfuric acid hydrolysis on the thermal degradation behavior of bacterial cellulose[J]. Biomacromolecules, 2004, 5(5): 1671-1677.

[26] Abitbol T, Kloser E, Gray D G. Estimation of the surface sulfur content of cellulose nanocrystals prepared by sulfuric acid hydrolysis[J]. Cellulose, 2013, 20(2): 785-794.

[27] Araki J, Wada M, Kuga S, et al. Birefringent glassy phase of a cellulose microcrystal suspension[J]. Langmuir, 2000, 16 (6): 2413-2415.

[28] Camarero Espinosa S, Kuhnt T, Foster E J, et al. Isolation of thermally stable cellulose nanocrystals by phosphoric acid hydrolysis[J]. Biomacromolecules. 2013, 14(4): 1223-1230.

[29] Sadeghifar H, Filpponen I, Clarke S P, et al. Production of cellulose nanocrystals using hydrobromic acid and click reactions on their surface[J]. Journal of Materials Science,

2011, 46 (22): 7344-7355.

[30] Edwards J V, Prevost N T, French A D, et al. Kinetic and structural analysis of fluorescent peptides on cotton cellulose nanocrystals as elastase sensors[J]. Carbohydrate Polymers, 2015, 116: 278-285.

[31] JaušovecD, VogrinčičR, Kokol V. Introduction of aldehyde vs. carboxylic groups to cellulose nanofibers using laccase/TEMPO mediated oxidation[J]. Carbohydrate Polymers, 2015, 116: 74-85.

[32] Garcia-Astrain C, González K, Gurrea T, et al. Maleimide-grafted cellulose nanocrystals as cross-linkers for bionanocomposite hydrogels[J]. Carbohydrate Polymers, 2016, 149: 94-101.

[33] De Menezes A J, Siqueira G, Curvelo A A S, et al. Extrusion and characterization of functionalized cellulose whiskers reinforced polyethylene nanocomposites[J]. Polymer, 2009, 50(19): 4552-4563.

[34] Grubbström G, Holmgren A, Oksman K. Silane-crosslinking of recycled low-density polyethylene/wood composites[J]. Composites Part A: Applied Science and Manufacturing, 2010, 41(5): 678-683.

[35] Habibi Y, Hoeger I, Kelley S S, et al. Development of langmuir-schaeffer cellulose nanocrystal monolayers and their interfacial behaviors[J]. Langmuir, 2010, 26(2): 990-1001.

[36] Thielemans W, Belgacem M N, Dufresne A. Starch nanocrystals with large chain surface modifications[J]. Langmuir, 2006, 22(10): 4804-4810.

[37] Eyley S, Thielemans W. Surface modification of cellulose nanocrystals[J]. Nanoscale, 2014, 6(14): 7764-7779.

[38] Dong S, Roman M. Fluorescently labeled cellulose nanocrystals for bioimaging applications[J]. Journal of American Chemical Society, 2007, 129(45): 13810-13811.

[39] Zoppe J O, Peresin M S, Habibi Y, et al. Reinforcing poly(epsilon-caprolactone) nanofibers with cellulose nanocrystals[J]. ACS Applied Materials & Interfaces, 2009, 1(9): 1996-2004.

[40] Angellier H, Molina-Boisseau S, Dufresne A. Mechanical properties of waxy maize starch nanocrystal reinforced natural rubber[J]. Macromolecules, 2005, 38(22): 9161-9170.

[41] Yang H, Tejado A, Alam N, et al. Films prepared from electrosterically stabilized nanocrystalline cellulose[J]. Langmuir, 2012, 28(20): 7834-7842.

[42] Brioude M M, Roucoules V, Haidara H, et al. Role of Cellulose nanocrystals on the microstructure of maleic anhydride plasma polymer thin films[J]. ACS Applied Materials & Interfaces, 2015, 7(25): 14079-14088.

[43] Qi H, Chang C, Zhang L. Properties and applications of biodegradable transparent and photoluminescent cellulose films prepared via a green process[J]. Green Chemistry, 2009, 11(2): 177-184.

[44] Tummala G K, Felde N, Gustafsson S, et al. Light scattering in poly(vinyl alcohol) hydrogels reinforced with nanocellulose for ophthalmic use[J]. Optical Materials Express, 2017, 7(8): 2824-2837.

[45] Morandi G, Thielemans W. Synthesis of cellulose nanocrystals bearing photocleavable grafts by ATRP[J]. Polymer Chemistry, 2012, 3(6): 1402-1407.

[46] Qu D, Zhang J, Chu G, et al. Chiral fluorescent films of gold nanoclusters and photonic cellulose with modulated fluorescence emission[J]. Journal of Materials Chemistry C, 2016, 4(9): 1764-1768.

[47] Thérien-Aubin H, Lukach A, Pitch N, et al. Structure and properties of composite films formed by cellulose nanocrystals and charged latex nanoparticles[J]. Nanoscale, 2015, 7(15): 6612-6618.

[48] Song J, Fu G, Cheng Q, et al. Bimodal mesoporous silica nanotubes fabricated by dual templates of CTAB and bare nanocrystalline cellulose[J]. Industrial & Engineering Chemistry Research, 2013, 53(2): 708-714.

[49] Maeda H, Nakajima M, Hagiwara T, et al. Bacterial cellulose/silica hybrid fabricated by mimicking biocomposites[J]. Journal of Materials Science, 2006, 41 (17): 5646-5656.

[50] Seabra A B, Bernardes J S, Favaro W J, et al. Cellulose nanocrystals as carriers in medicine and their toxicities: a review[J]. Carbohydrate Polymers, 2018, 181: 514-527.

[51] Viet D, Beck-Candanedo S, Gray D G. Dispersion of cellulose nanocrystals in polar organic solvents[J]. Cellulose, 2006, 14(2): 109-113.

[52] Aylott J W. Optical nanosensors—an enabling technology for intracellular measurements[J]. The Analyst, 2003, 128 (4): 309-312.

[53] Helbert W, Chanzy H, Husum T L, et al. Fluorescent cellulose microfibrils as substrate for the detection of cellulase activity[J]. Biomacromolecules, 2003, 4(3): 481-487.

[54] Ferreira L F V, Cabral P V, Almeida P, et al. Ultraviolet visible absorption, luminescence, and X-ray photoelectron spectroscopic studies of a rhodamine dye covalently bound to microcrystalline cellulose[J]. Macromolecules, 1998, 31 (12): 3936-3944.

[55] Nawaz H, Tian W, Zhang J, et al. Cellulose-Based Sensor Containing Phenanthroline for the Highly Selective and Rapid Detection of Fe(2+) ions with naked eye and fluorescent dual modes[J]. ACS Applied Materials & Interfaces, 2018, 10(2): 2114-2121.

[56] Xu W, Mu L, Miao R, et al. Fluorescence sensor for Cu(II) based on R6G derivatives modified silicon nanowires[J]. Journal of Luminescence, 2011, 131(12): 2616-2620.

[57] Bag B, Pal A. Rhodamine-based probes for metal ion-

induced chromo-/fluorogenic dual signaling and their selectivity towards Hg(II) ion[J]. Org Biomol Chem, 2011, 9 (12): 4467-4480.

[58] Panda S, Pati P B, Zade S S. Twisting (conformational changes)-based selective 2D chalcogeno podand fluorescent probes for Cr(III) and Fe(II)[J]. Chemical Communications, 2011, 47(14): 4174-4176.

[59] De Silva A P, Gunaratne H Q, Gunnlaugsson T, et al. Signaling recognition events with fluorescent sensors and switches[J]. Chemical Reviews, 1997, 97(5): 1515-1566.

[60] Li L, Pan S S, Dou X C, et al. Direct electrodeposition of ZnO nanotube arrays in anodic alumina membranes[J]. Journal of Physical Chemistry C, 2007, 111(20): 7288-7291.

[61] Chen J, Zhou Z, Chen Z, et al. A fluorescent nanoprobe based on cellulose nanocrystals with porphyrin pendants for selective quantitative trace detection of Hg^{2+}[J]. New Journal of Chemistry, 2017, 41(18): 10272-10280.

[62] Zhang L, Li Q, Zhou J, et al. Synthesis and photophysical behavior of pyrene-bearing cellulose nanocrystals for Fe^{3+} sensing[J]. Macromolecular Chemistry and Physics, 2012, 213(15): 1612-1617.

[63] Saito T, Kimura S, Nishiyama Y, et al. Cellulose nanofibers prepared by TEMPO-mediated oxidation of native cellulose[J]. Biomacromolecules, 2007, 8(8): 2485-2491.

[64] Follain N, Marais M F, Montanari S, et al. Coupling onto surface carboxylated cellulose nanocrystals[J]. Polymer, 2010, 51(23): 5332-5344.

[65] Okita Y, Saito T, Isogai A. Entire surface oxidation of various cellulose microfibrils by TEMPO-mediated oxidation[J]. Biomacromolecules, 2010, 11(6): 1696-1700.

[66] Da Silva Perez D, Montanari S, Vignon M R. TEMPO-mediated oxidation of cellulose III[J]. Biomacromolecules, 2003, 4(5): 1417-1425.

[67] Mangalam A P, Simonsen J, Benight A S. Cellulose/DNA hybrid nanomaterials[J]. Biomacromolecules, 2009, 10 (3): 497-504.

[68] Kumari S, Chauhan G S. New cellulose-lysine Schiff-base-based sensor-adsorbent for mercury ions[J]. ACS Applied Materials & Interfaces, 2014, 6(8): 5908-5917.

[69] Leung A C, Hrapovic S, Lam E, et al. Characteristics and properties of carboxylated cellulose nanocrystals prepared from a novel one-step procedure[J]. Small, 2011, 7(3): 302-305.

[70] Shibata I, Yanagisawa M, Saito T, et al. SEC-MALS analysis of cellouronic acid prepared from regenerated cellulose by TEMPO-mediated oxidation[J]. Cellulose, 2006, 13(1): 73-80.

[71] Shibata I, Isogai A. Nitroxide-mediated oxidation of cellulose using TEMPO derivatives: HPSEC and NMR analyses of the oxidized products[J]. Cellulose, 2003, 10 (4): 335-341.

[72] Saito T, Yanagisawa M, Isogai A. TEMPO-mediated oxidation of native cellulose: SEC-MALLS analysis of water-soluble and -insoluble fractions in the oxidized products[J]. Cellulose, 2005, 12(3): 305-315.

[73] Lin N, Bruzzese C, Dufresne A. TEMPO-oxidized nanocellulose participating as crosslinking aid for alginate-based sponges[J]. ACS Applied Materials & Interfaces, 2012, 4(9): 4948-4959.

[74] Lin N, Dufresne A. Physical and/or chemical compatibilization of extruded cellulose nanocrystal reinforced polystyrene nanocomposites[J]. Macromolecules, 2013, 46(14): 5570-5583.

[75] Mascheroni E, Rampazzo R, Ortenzi M A, et al. Comparison of cellulose nanocrystals obtained by sulfuric acid hydrolysis and ammonium persulfate to be used as coating on flexible food-packaging materials[J]. Cellulose, 2016, 23(1): 779-793.

[76] Abitbol T, Marway H S, Kedzior S A, et al. Hybrid fluorescent nanoparticles from quantum dots coupled to cellulose nanocrystals[J]. Cellulose, 2017, 24(3): 1287-1293.

[77] Grate J W, Mo K F, Shin Y, et al. Alexa Fluor-labeled fluorescent cellulose nanocrystals for bioimaging solid cellulose in spatially structured microenvironments[J]. Bioconjugate Chemistry, 2015, 26(3): 593-601.

[78] Huang J L, Li C J, Gray D G. Cellulose nanocrystals incorporating fluorescent methylcoumarin groups[J]. ACS Sustainable Chemistry & Engineering, 2013, 1(9): 1160-1164.

[79] Zhou Y, Jin Q, Hu X, et al. Heavy metal ions and organic dyes removal from water by cellulose modified with maleic anhydride[J]. Journal of Materials Science, 2012, 47(12): 5019-5029.

[80] Zhang Y J, Ma X Z, Huang J, et al. Fabrication of fluorescent cellulose nanocrystal via controllable chemical modification towards selective and quantitative detection of Cu(II) ion[J]. Cellulose, 2018, 1-12.

[81] Sîrbu E, Eyley S, Thielemans W. Coumarin and carbazole fluorescently modified cellulose nanocrystals using a one-step esterification procedure[J]. The Canadian Journal of Chemical Engineering, 2016, 94(11): 2186-2194.

[82] Gorgieva S, Vivod V, Maver U, et al. Internalization of (bis) phosphonate-modified cellulose nanocrystals by human osteoblast cells[J]. Cellulose, 2017, 24(10): 4235-4252.

[83] Hassan M L, Moorefield C M, Elbatal H S, et al. New metallo-supramolecular terpyridine-modified cellulose functional nanomaterials[J]. Journal of Macromolecular

Science, Part A, 2012, 49(4): 298-305.

[84] Wu W, Li J, Liu W, et al. Temperature-sensitive, fluorescent poly(N-Isopropyl-acrylamide)-grafted cellulose nanocrystals for drug release[J]. Bioresources, 2016, 11(3): 7026-7035.

[85] Wu W, Huang F, Pan S, et al. Thermo-responsive and fluorescent cellulose nanocrystals grafted with polymer brushes[J]. Journal of Materials Chemistry A, 2015, 3(5): 1995-2005.

[86] Yuan W, Wang C, Lei S, et al. Ultraviolet light-, temperature- and pH-responsive fluorescent sensors based on cellulose nanocrystals[J]. Polymer Chemistry, 2018, 9 (22): 3098-3107.

[87] Chen L, Cao W, Grishkewich N, et al. Synthesis and characterization of pH-responsive and fluorescent poly (amidoamine) dendrimer-grafted cellulose nanocrystals[J]. Journal of Colloid & Interface Science, 2015, 450(12): 101-108.

[88] Eyley S, Thielemans W. Imidazolium grafted cellulose nanocrystals for ion exchange applications[J]. Chemical Communications, 2011, 47(14): 4177-4179.

[89] Parsamanesh M, Tehrani A D. Synthesize of new fluorescent polymeric nanoparticle using modified cellulose nanowhisker through click reaction[J]. Carbohydrate Polymers, 2016, 136: 1323-1331.

[90] Abitbol T, Palermo A, Moran-Mirabal J M, et al. Fluorescent labeling and characterization of cellulose nanocrystals with varying charge contents[J]. Biomacromolecules, 2013, 14 (9): 3278-3284.

[91] Zhao L, Li W, Plog A, et al Multi-responsive cellulose nanocrystal-rhodamine conjugates: an advanced structure study by solid-state dynamic nuclear polarization (DNP) NMR[J]. Physical Chemistry Chemical Physics, 2014, 16 (47): 26322-26329.

[92] Guo J, Liu D, Filpponen I, et al. Photoluminescent hybrids of cellulose nanocrystals and carbon quantum dots as cytocompatible probes for in vitro bio-imaging[J]. Biomacromolecules, 2017, 18(7): 2045-2055.

[93] Filpponen I, Sadeghifar H, Argyropoulos D S. Photoresponsive cellulose nanocrystals[J]. Nanomaterials and Nanotechnology, 2011, 1(1): 34-43.

[94] Colombo L, Zoia L, Violatto M B, et al. Organ distribution and bone tropism of cellulose nanocrystals in living mice[J]. Biomacromolecules, 2015, 16(9): 2862-2871.

[95] Yang Q, Pan X. A facile approach for fabricating fluorescent cellulose[J]. Journal of Applied Polymer Science, 2010, 117(6): 3639-3644.

[96] Cai C, Wei B, Jin Z, et al. Facile method for fluorescent labeling of starch nanocrystal[J]. ACS Sustainable Chemistry & Engineering, 2017, 5(5): 3751-3761.

[97] Nielsen L J, Eyley S, Thielemans W, et al. Dual fluorescent labelling of cellulose nanocrystals for pH sensing[J]. Chemical Communications, 2010, 46(47): 8929-8931.

[98] Tang L, Li T, Zhuang S, et al. Synthesis of pH-sensitive fluorescein grafted cellulose nanocrystals with an amino acid spacer[J]. ACS Sustainable Chemistry & Engineering, 2016, 4(9): 4842-4849.

[99] Mahmoud K A, Mena J A, Male K B, et al. Effect of surface charge on the cellular uptake and cytotoxicity of fluorescent labeled cellulose nanocrystals[J]. ACS Applied Materials & Interfaces, 2010, 2(10): 2924-2932.

[100] Ding Q, Zeng J, Wang B, et al. Influence of binding mechanism on labeling efficiency and luminous properties of fluorescent cellulose nanocrystals[J]. Carbohydrate Polymers, 2017, 175: 105-112.

[101] Khabibullin A, Alizadehgiashi M, Khuu N, et al. Injectable shear-thinning fluorescent hydrogel formed by cellulose nanocrystals and graphene quantum dots[J]. Langmuir, 2017, 33(43): 12344-12350.

[102] Zhang L, Zhou J, Zhang L. Synthesis and fluorescent properties of carbazole-substituted hydroxyethyl celluloses[J]. Macromolecular Chemistry and Physics, 2012, 213(1): 57-63.

[103] Hassan M L, Moorefield C M, Elbatal H S, et al. Fluorescent cellulose nanocrystals via supramolecular assembly of terpyridine-modified cellulose nanocrystals and terpyridine-modified perylene[J]. Materials Science and Engineering: B, 2012, 177(4): 350-358.

[104] Harrisson S, Drisko G L, Malmstrom E, et al. Hybrid rigid/soft and biologic/synthetic materials: polymers grafted onto cellulose microcrystals[J]. Biomacromolecules, 2011, 12(4): 1214-1223.

[105] Way A E, Hsu L, Shanmuganathan K, et al. pH-responsive cellulose nanocrystal gels and nanocomposites[J]. ACS Macro Letters, 2012, 1(8): 1001-1006.

[106] Akhlaghi S P, Berry R C, Tam K C. Surface modification of cellulose nanocrystal with chitosan oligosaccharide for drug delivery applications[J]. Cellulose, 2013, 20(4): 1747-1764.

[107] Tang Y, Yang S, Zhang N, et al. Preparation and characterization of nanocrystalline cellulose via low-intensity ultrasonic-assisted sulfuric acid hydrolysis[J]. Cellulose, 2013, 21(1): 335-346.

[108] Gong B, Liu W, Chen X, et al. Stabilizing alkenyl succinic anhydride (ASA) emulsions with starch nanocrystals and fluorescent carbon dots[J]. Carbohydrate Polymers, 2017, 165: 13-21.

[109] Figueira F, Farinha A S, Muteto P V, et al. [28] Hexaphyrin derivatives for anion recognition in organic and aqueous media[J]. Chemical Communications, 2016,

52(10): 2181-2184.

[110] Shamsipur M, Sadeghi M, Beyzavi M H, et al. Development of a novel fluorimetric bulk optode membrane based on meso-tetrakis(2-hydroxynaphthyl) porphyrin (MTHNP) for highly sensitive and selective monitoring of trace amounts of Hg^{2+} ions[J]. Materials Science and Engineering: C, 2015, 48: 424-433.

[111] Motreff N, Le Gac S, Luhmer M, et al. Formation of a dinuclear mercury(II) complex with a regular bis-strapped porphyrin following a tunable cooperative process[J]. Angewandte Chemie International Edition, 2011, 50(7): 1560-1564.

[112] Suijkerbuijk B M, Klein Gebbink R J. Merging porphyrins with organometallics: synthesis and applications[J]. Angewandte Chemie International Edition, 2008, 47(39): 7396-7421.

[113] Caselli M. Porphyrin-based electrostatically self-assembled multilayers as fluorescent probes for mercury (II) ions: a study of the adsorption kinetics of metal ions on ultrathin films for sensing applications[J]. RSC Advances, 2015, 5(2): 1350-1358.

[114] Lv J, Ouyang C, Yin X, et al. Reversible and highly selective fluorescent sensor for mercury(II) based on a water-soluble poly(para-phenylene)s containing thymine and sulfonate moieties[J]. Macromolecular Rapid Communications, 2008, 29(19): 1588-1592.

[115] Hu Z Q, Feng Y C, Huang H Q, et al. Fe^{3+}-selective fluorescent probe based on rhodamine B and its application in bioimaging[J]. Sensors and Actuators B: Chemical, 2011, 156(1): 428-432.

[116] Kumar R, Nandi G C, Verma R K, et al. A facile approach for the synthesis of 14-aryl- or alkyl-14H-dibenzo[a, j] xanthenes under solvent-free condition[J]. Tetrahedron Letters, 2010, 51(2): 442-445.

[117] Aamer K A, Tew G N. Supramolecular polymers containing terpyridine-metal complexes in the side chain[J]. Macromolecules, 2007, 40(8): 2737-2744.

[118] Morsali A, Monfared H H, Morsali A. Syntheses and characterization of nano-scale of the Mn (II) complex with 4′-(4-pyridyl)-2,2′:6′,2″-terpyridine (pyterpy): the influence of the nano-structure upon catalytic properties[J]. Inorganica Chimica Acta, 2009, 362(10): 3427-3432.

[119] Chiper M, Hoogenboom R, Schubert U S. New terpyridine macroligands as potential synthons for supramolecular assemblies[J]. European Polymer Journal, 2010, 46(2): 260-269.

[120] Yeung C T, Lee W S, Tsang C S, et al. Chiral-symmetric 2,2′:6′,2″-terpyridine ligands: synthesis, characterization, complexation with copper(II), rhodium(III) and ruthenium(II) ions and use of the complexes in catalytic cyclopropanation of styrene[J]. Polyhedron, 2010, 29(5): 1497-1507.

[121] Kamyabi M A, Narimani O, Monfared H H. Electrocatalytic oxidation of hydrazine using glassy carbon electrode modified with carbon nanotube and terpyridine manganese(II) complex[J]. Journal of Electroanalytical Chemistry, 2010, 644(1): 67-73.

[122] Hornig S, Manners I, Newkome G R, et al. Metal-containing and metallo-supramolecular polymers and materials[J]. Macromolecular Rapid Communications, 2010, DOI:10.1002/marc.201000196.

[123] Chiper M, Hoogenboom R, Schubert U S. Toward main chain metallo-terpyridyl supramolecular polymers: “the metal does the trick”[J]. Macromolecular Rapid Communications, 2009, 30(8): 565-578.

[124] Goncalves A C, Luis Capelo J, Lodeiro C, et al. A selective emissive chromogenic and fluorogenic seleno-coumarin probe for Cu^{2+} detection in aprotic media[J]. Photochemical & Photobiological Sciences, 2017, 16(7): 1174-1181.

[125] Karaoglu K, Yilmaz F, Mentese E. A new fluorescent “Turn-Off” coumarin-based chemosensor: synthesis, structure and Cu-selective fluorescent sensing in water samples[J]. Journal of Fluorescence, 2017, 27(4): 1293-1298. PBM